Comprehensive Sensitivity and Cross-Factor Variance Analysis-Based Multi-Objective Design Optimization of a 3-DOF Hybrid Magnetic Bearing

Zhijia Jin[1], Xiaodong Sun[1], Yingfeng Cai[1], Jianguo Zhu[2], Gang Lei[3], and Youguang Guo[3]
[1]Automotive Engineering Research Institute, Jiangsu University, Zhenjiang 212013, China
[2] School of Electrical and Information Engineering, University of Sydney, Sydney, NSW2006, Australia
[3]School of Electrical and Data Engineering, University of Technology Sydney, NSW 2007, Australia

Multi-degree-of-freedom (MDOF) magnetic bearings have been widely investigated and designed for various applications. However, a new design magnetic bearing cannot be directly used without optimization due to the not relatively excellent performance. Besides, there may be a lack of consideration of the interaction of parameters in the design process. Hence, in this paper, a three-degree-of freedom hybrid magnetic bearing (THMB) is optimized as an example. First, a comprehensive sensitivity analysis is carried out to show the relationship between the parameters and optimization objectives in detail. Second, a cross-factor variance analysis is considered due to the possibility of parameter interaction. And then, a hierarchical multi-objective optimization structure is used with Kriging Model and non-dominated Sorting Genetic Algorithm II (NSGA II). The simulation results verify the validity of the proposed method, and the prototype is under manufacture for further evaluation.

***Index Terms*—Three-degree-of freedom hybrid magnetic bearing (THMB); multi-objective optimization, comprehensive sensitivity analysis; cross-factor variance analysis, Kriging Model.**

I. Introduction

HYBRID magnetic bearings (HMBs) have found their performance fields such as control moment gyros, high-speed motors, flywheel energy storage system and compressors [1-3]. HMB combines the advantages of both AMB and PMB manifesting in lower loss than AMB, easier controllability and higher stiffness than PMB [4]. Besides, the demand of multi-degree-of-freedom (MDOF) magnetic bearings is also increasing currently.

To reduce the axial length and increase the critical speed of the magnetic bearing system, some novel three-degree-of-freedom hybrid magnetic bearings (THMB) are designed recently [5-7]. These special structures can provide both radial and axial suspension forces independently [8]. However, little effort has been spent optimizing the THMBs. In fact, because of the existence of permanent magnets and the complexity of magnetic circuit, the extent to which performances are affected by parameters is unclear. Therefore, a multi-objective optimization is difficult but necessary for wide application prospects.

As for the multi-objective optimization of THMBs, the effectiveness of optimization usually depends on the following points. First is the accurate sensitivity analysis between the parameters and objectives, objectives and objectives and even objectives and constrains. The sensitivity analysis directly determines the specific form of the optimized structure. Additionally, a case may occur that two parameters may be highly correlated with each other while one has a high correlation coefficient, and another has a low correlation coefficient. This may not be taken into consideration in many optimizations while it does affect.

Corresponding author: X. Sun (e-mail: xdsun@ujs.edu.cn)

The second point is the optimization strategy. As the number of parameters increases, the computational cost of the finite element analysis (FEA) increases dramatically [9, 10]. For example, establishing an optimization model with 4 parameters and 4 levels needs to run 256 models, that may be still acceptable at a single level. However, one more parameter added requires an additional 768 models. In this case, a multi-level structure is essential. As for a THMB, the number of parameters is quite large because both radial and axial suspension forces are considered.

To solve the above two problems about the optimization of MDOF magnetic bearings, in this paper, a typical THMB is taken as an optimization example. The multi-level optimization structure is determined by the results of the comprehensive sensitivity analysis and the cross-factor variance analysis. In addition, the Kriging Model [11] is applied as the optimization model and the non-dominated Sorting Genetic Algorithm II (NSGA II) [12] is used to global search due to its effectiveness in optimization problems.

The remaining of this paper is divided as follows. In section II, topology and initial design parameters of the THMB are given. In Section III, optimization objectives, complete sensitivity analysis and the multi-objective optimization structure are explained in particular. Section IV shows the simulation results and discusses in detail. Finally, the conclusions are drawn in Section V.

II. The Structure of the HMB

The three-dimensional structure of the THMB is shown in Fig. 1. As it can be seen, the THMB mainly contains a rotor, an inner stator, an outer stator and four PMs. The PMs are magnetized by radial direction in order to provide stable bias passive magnetic loop. There is a radial air gap between the rotor and the inner stator and an axial air gap between the rotor and the outer stator. Besides, the structural dimension parameters are given in Table I

As for the principle, it works by the interaction between the bias passive magnetic loop and magnetic loop excited by coils, both the radial and axial direction. The magnetic density in one air gap is stronger than that in the opposite air gap so that the maglev force is generated.

TABLE I
INITIAL DESIGN AND RANGES OF THE PARAMETERS

Symbol	Quantity	Initial value	Ranges
L_{os}	thickness of piece	4mm	3-6mm
L_s	thickness of stator	10.5mm	8.4-12.6mm
G_z	height of axial gap	0.5mm	0.3-0.65mm
Gus	height of radial gap	0.5mm	0.3-0.65mm
H_z	thickness of inner ring column	5.3mm	4-6.5mm
H_t	stator tooth width	41.7mm	32.8-49.2mm
H_{PM}	thickness of PM	12mm	9.6-14.4mm
H_r	thickness of rotor	15mm	12-18mm
H_{is}	inner stator yoke width	15mm	12-18mm
H_{os}	thickness of outer ring column	4mm	3-6mm

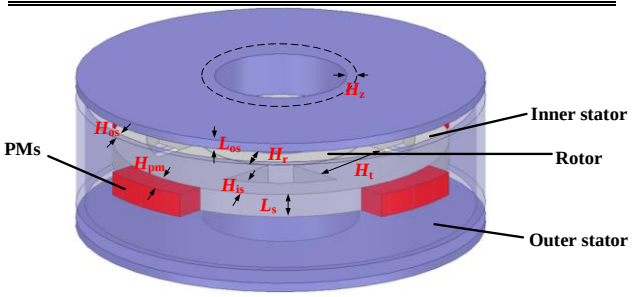

(a)

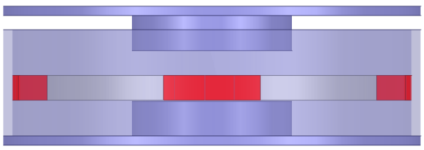

(b)

Fig. 1. The three-dimensional structure of the THMB. (a)overall view (b)horizontal view.

III. MULTI-OBJECTIVE OPTIMIZATION

A. Objectives Selection

$$\min\begin{cases} f_1(x_1,x_2,\cdots x_n) = -F_x \\ f_2(x_1,x_2,\cdots x_n) = -F_z \\ f_3(x_1,x_2,\cdots x_n) = P \end{cases} \tag{1}$$

$$\begin{cases} g(x_1,x_2\cdots x_n) = R_x - R_r \le 0 \\ g(x_1,x_2\cdots x_n) = R_z - R_a \le 0 \\ g(x_1,x_2\cdots x_n) = L - L_a \le 0 \\ g(x_1,x_2\cdots x_n) = G - G_{\max} \le 0 \end{cases} \tag{2}$$

For a THMB, compared with the traditional radial magnetic bearing, the optimization objectives and constraints also increase with the complexity of the structure, and the most intuitive is the axial suspension force, ripple and the axial length. Besides, due to the huge differences of the structures and magnetic circuits, the core loss of the THMB also differs. And generally, reliable suspension forces are critical to a THMB. Therefore, in this paper, the radial and axial suspension force, and the core loss are selected as the optimization objectives. And the objectives and constraints are shown in (1) and (2), where F_x and F_z are maximum radial and axial suspension forces, respectively. P is the minimum core loss. R_x and R_z are practical ripples, and R_r and R_a are constraint ripples. L and L_a are practical and constraint axial lengths. G and G_{max} are practical and constraint magnetic density.

B. Comprehensive Sensitivity Analysis

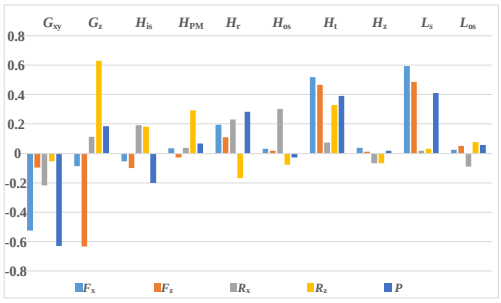

Fig. 2. Comprehensive sensitivity analysis.

A comprehensive sensitivity analysis method is adopted to evaluate the effect of the parameters on the optimization objectives, and it is necessary after determining the objectives. Since each parameter may have different influence on the different objectives, in this paper, the Pearson correlational coefficient is used to perform the sensitivity analysis. And it can be calculated as (3).

$$\rho_{Q_i,R_i} = \frac{N\sum Q_i R_i - \sum Q_i \sum R_i}{\sqrt{N\sum Q_i^2 - (\sum Q_i)^2}\sqrt{N\sum R_i^2 - (\sum R_i)^2}} \tag{3}$$

where R_i is the ith optimization objective, Q_i is the design parameters, and N is sample size.

Thus, the sensitivity of each parameter on the objectives is shown in Fig. 2. It can be noted that the sensitivity of each parameter to the objectives varies greatly, and G_{xy}, G_z, H_t and L_s have relatively great influence on single or multiple objectives, which can be considered as the high sensitive parameters. H_z and L_{os} have little effect on the objectives basically, therefore, they will be not considered in the optimization process. The remaining parameters have some effect on the objectives or constraints, determining as the general sensitive parameters.

C. Cross-Factor Variance Analysis

If two parameters have huge correlation with each other while the sensitivities of one objective differs seriously. Usually, the single sensitivity analysis cannot find and solve such problem. Hence, a cross-factor variance analysis is needed.

Considering the parameter interactions, a new design of experiments (DOE) need to be carried out first which contains the interactions of parameters, and the interactions are considered as independent factors together with other single parameters. And the F-test result will be used to show the correlation effects.

TABLE II
SIGNIFICANT CROSS-FACTORS

Optimization objectives	F_x	F_z	P
Cross factors	(L_s ×G_{xy}) (L_s ×H_t) (L_s ×H_r)	(L_s ×H_{pm}) (L_s ×H_t)	(L_s ×H_t) (L_s ×H_r)

The analysis results are given in Table II. It can be noted that some cross factors have significant influence on the objectives, respectively. And most of single parameters in the results already have relatively huge sensitivity in the sensitivity analysis, except the H_{is}. Hence, it is necessary to classify it as a sensitive parameter.

D. *Multi-objective optimization strategy*

As known that the computational cost will be really considerable if all the parameters are considered simultaneously in a same level. Therefore, it's important to find a suitable optimization structure for the THMB to be optimized. According to the results of the above analysis, the parameters can be divided into three levels. Thus, a double-level optimization structure is proposed and the flowchart is shown in Fig. 3.

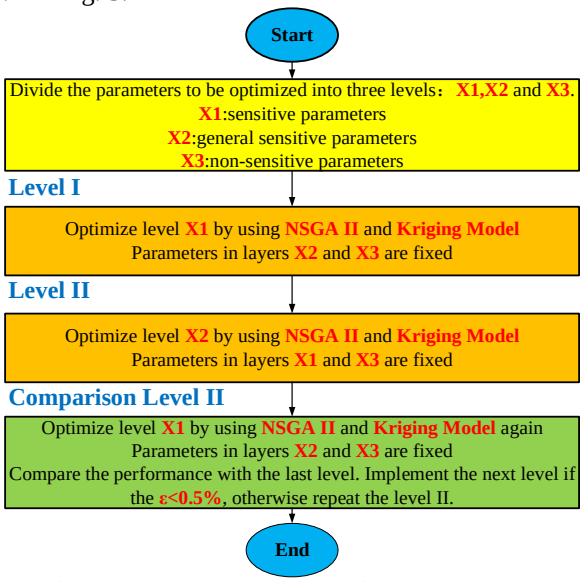

Fig. 3. The flowchart of the multi-objective performance optimization.

First, the parameters can be divided into three levels, X1, X2 and X3. The parameters in X3 level are always fixed due to the small impact.

Second, the high sensitive parameters in X1 are optimized firstly, then the general sensitive parameters in X2. In the Level I optimization, the parameter values in level X1 (G_{xy}, G_z, H_t, L_s and H_{is}) are optimized and parameter values in level X2 (H_z and L_{os}) and level X3 (H_{PM}, L_{os}, H_z and H_{os}) are fixed. Similarly, in Level II optimization, the parameter values in level X2 (H_z and L_{os}) are optimized, and parameter values in level X1 (G_{xy}, G_z, H_t, L_s and H_{is}) and level X3 (H_{PM}, L_{os}, H_z and H_{os}) are fixed. Besides, in each optimization level, the Kriging Model is applied to establish the optimization model. Kriging Model is a semi-parameter model which is often used in optimization problems due to its fast and efficient modeling ability. Additionally, NSGA II is used for the global search.

Third, a comparison level is introduced as shown in Fig. 3. The optimization in level I will be done again after the level II is finished. An evaluation parameter ε is introduced to determine the optimization process, which can be expressed as:

$$\varepsilon = \max\left\{\left(\frac{F_{xIC}}{F_{xII}}, \frac{P_{II}}{P_{IC}}, \frac{F_{zIC}}{F_{zII}}\right)\times 100\%\right\}, \tag{4}$$

where the subscript IC and II denote the optimization results in comparison level optimization and level II optimization, respectively. If the ε is less than 0.5%, the optimization is finished. Otherwise, return to level II.

IV. RESULTS AND VERIFICATION

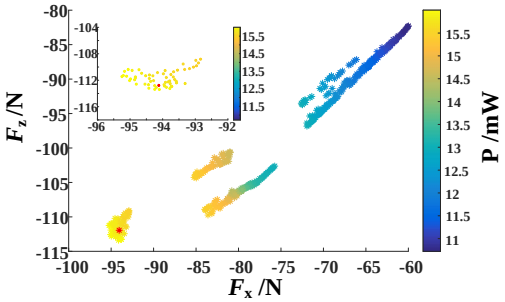

Fig. 4. Pareto solutions of Level I optimization.

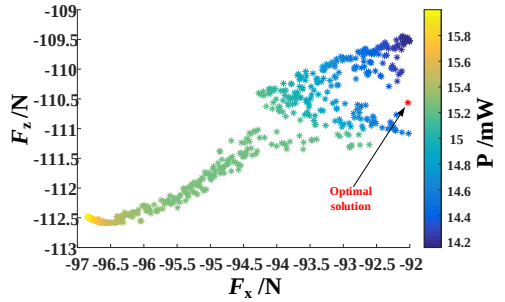

Fig. 5. Pareto solutions of Level II optimization.

Fig. 4 shows the pareto solutions of Level I optimization. As shown, the maximum radial and axial suspension force can reach 95.5N and 114N, respectively. And the minimum core loss is 11mW. To select a most suitable optimal solution in Level I optimization, a demand function is needed. A commonly used demand function can be expressed as follows:

$$f(k) = \omega_1 \frac{F_z}{F_{zi}} + \omega_2 \frac{F_x}{F_{xi}} + \omega_3 \frac{P_i}{P} \tag{5}$$

where F_{xi}, F_{zi} and P_i are initial radial and axial suspension force and core loss, respectively; ω_1, ω_2 and ω_3 are weight coefficients which are determined by the performance ranges after homogenization since there are no optimization requirements in advance. Then, ω_1, ω_2 and ω_3 are set as 5.46, 6.96 and 6.25, respectively. According to the calculation results, Table III shows the optimal value. And the optimal solution is marked in Fig. 4.

TABLE III
OPTIMAL SOLUTION OF LEVEL I

G_{xy}	G_z	L_s	H_{is}	H_t
0.4mm	0.5mm	10.53mm	15.67mm	49.2mm
Function value		F_x	F_z	P

24.73	94.2N	112.8N	15.8mW

Similarly, the pareto solutions of Level II optimization are shown in Fig. 5. It can be clearly noted that the ranges of optimal solution are obviously reduced after the determination of the parameters in X1. The maximum radial suspension force can reach 97N while the optimal improvement of the axial suspension force and core loss are not very obvious in this level.

The same method that selects the optimal solution can refer to equation (4). And in this level, ω_1, ω_2 and ω_3 are reset as 9.48, 9.64 and 8.88, respectively. The optimal solution value is given in Table IV.

TABLE IV
OPTIMAL SOLUTION OF LEVEL II

H_{pm}	H_r	H_{os}	
14.40mm	13.61mm	3.78mm	
Function value	F_x	F_z	P
27.47	92.03N	110.56N	14.30mW

And then, the parameters in X2 and X3 are fixed again, and the Level I optimization is repeated. After verification, the above optimization results meet the requirements that ε<0.5%. Therefore, according to the optimization results, the radial and axial suspension force are improved by 4.78% and 67.77%, respectively, and the core loss is reduced by 2.43mW. It can be noted that the axial suspension force particularly increases while the other two objectives have the general optimization effect. This may be caused by the position of the initial parameters. Meanwhile, it proves that there is huge room for improvement of the THMB performances after the initial design.

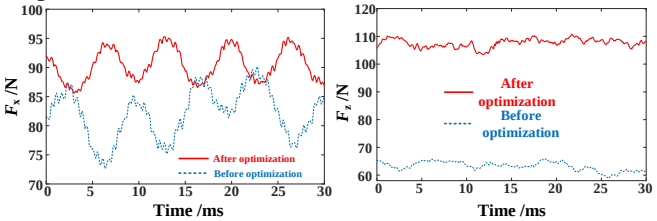

(a) (b)

Fig.6. The radial and axial suspension forces before and after optimization (a) radial suspension force (b) axial suspension force.

Fig. 6 shows the comparison results before and after optimization in finite element simulation. As shown, the performance improvements are basically consistent with those of optimization results. That can reflect the effectiveness of optimization. However, the specific simulation values are slight less than optimization values, which are about 1-2N. The reasons may be the insufficient number of sampling points or that the model used is not accurate enough which can be further studied.

V. CONCLUSION

In this paper, a THMB which generates the radial and axial suspension force simultaneously is optimized. Because of the complexity of MDOF magnetic bearing structure, a comprehensive sensitivity analysis is first performed to clarify the relationship between parameters and targets. Besides, to avoid the influence of cross factors on the optimal results, a cross-factor variance analysis is carried out. A double-level multi-objective optimization structure is applied to improve the optimization efficiency and reduce the computational cost. And the Kriging Model and NSGA II are used in each level. According to the optimization results, the radial and axial suspension force are improved by 4.78% and 67.77%, respectively, and the core loss is reduced by 2.43mW. In short, it proves that the performances of the THMB can be highly improved after the optimization design.

ACKNOWLEDGMENT

This work was supported by the National Natural Science Foundation of China under Projects 51875261 and 51875255, the National Key Research and Development Program of China under Project 2017YFB0102603, the Natural Science Foundation of Jiangsu Province of China under Projects BK20180046, BK20170071, and BK20180100, the “Qinglan project” of Jiangsu Province, the Six Categories Talent Peak of Jiangsu Province under Project 2018-TD-GDZB-022, and Key Project for the Development of Strategic Emerging Industries of Jiangsu Province under Project 2016-1094.

REFERENCES

[1] X. Sun, L. Chen, and Z. Yang, “Overview of bearingless permanentmagnet synchronous machines,” *IEEE Trans. Ind. Electron.*, vol. 60, no. 12, pp. 5528-5538, Dec. 2013.

[2] Z. Shi, X. Sun, G. Lei, Z. Yang, Y. Guo, and J. Zhu. “Analysis and optimization of radial force of permanent magnet synchronous Hub motors,” *IEEE Trans. Magn.*, vol. 56, no. 2, Feb. 2020, Art. no.: 7508804.

[3] X. Sun, Z. Jin, S. Wang, Z. Yang, K. Li, Y. Fan and L. Chen, “Performance improvement of torque and suspension force for a novel five-phase BFSPM machine for flywheel energy storage systems,” *IEEE Trans. Appl. Supercond.*, vol. 29, no. 2, Mar. 2019, Art. no. 0601505.

[4] J. Sun, Z. Ju, C. Peng, Y. Le and H. Ren “A novel 4-dof hybrid magnetic bearing for DGMSCMG”, *IEEE Trans. Ind. Electron.*, vol. 64, no. 3, pp. 2196-2204, Feb. 2017.

[5] Y. Le, J. Sun, and B. Han, “Modeling and design of 3-dof magnetic bearing for high-speed motor including eddy-current effects and leakage effects”, *IEEE Trans. Ind. Electron.*, vol. 63, no. 6, pp. 3656-3665, Jun. 2016.

[6] X. Sun, B. Su, L. Chen, Z. Yang, X. Xu, and Z. Shi, “Precise control of a four degree-of-freedom permanent magnet biased active magnetic bearing system in a magnetically suspended direct-driven spindle using neural network inverse scheme,” *Mech. Syst. Signal Process.*, vol. 88, pp. 36-48, 2017.

[7] J. Fang, J. Sun, H. Liu and J. Tang, “A novel 3-DOF axial hybrid magnetic bearing”, *IEEE Trans. Magn.*, Vol. 46, no. 12, pp. 4034-4045, Dec. 2010.

[8] B. Han, Q. Xu and Q. Yuan, “Multiobjective optimization of a combined radial-axial magnetic bearing for magnetically suspended compressor”, *IEEE Trans. Ind. Electron.*, vol. 63, no. 4, pp. 2284-2293, Feb. 2016.

[9] X. Sun, Z. Shi, G. Lei, Y. Guo, and J. Zhu, “Multi-objective design optimization of an IPMSM based on multilevel strategy,” *IEEE Trans. Ind. Electron.*, 2020, DOI: 10.1109/TIE.2020.2965463.

[10] K. Diao, X. Sun, G. Lei, Y. Guo, and J. Zhu, “Multiobjective system level optimization method for switched reluctance motor drive systems using finite element model,” *IEEE Trans. Ind. Electron.*, 2020, DOI: 10.1109/TIE.2019.2962483.

[11] Z. Shi, X. Sun, Y. Cai, and Z. Yang, “Robust design optimization of a five-phase PM hub motor for fault-tolerant operation based on Taguchi method,” *IEEE Trans. Energy Convers.*, 2020, DOI: 10.1109/TEC.2020.2989438.

[12] K. Deb, A. Pratap, S. Agarwal and T. Meyarivan, “A fast and elitist multi-objective genetic algorithm: NSGA-II.” *IEEE Trans Evol. Comput.*, vol. 6, no. 2, pp. 182–197, 2002.